Conducting states caused by a surface electric dipole in CrN(001) very thin films

Antía S. Botana,[1,2,*] Víctor Pardo,[1,2] Daniel Baldomir,[1,2] and Peter Blaha[3]

[1]*Departamento de Física Aplicada, Universidade de Santiago de Compostela, E-15782 Campus Sur s/n, Santiago de Compostela, Spain*

[2]*Instituto de Investigacións Tecnolóxicas, Universidade de Santiago de Compostela, E-15782 Campus Sur s/n, Santiago de Compostela, Spain*

[3]*Institute of Materials Chemistry, Vienna University of Technology, Getreidemarkt 9/165-TC, A-1060 Vienna, Austria*

(Received 29 November 2012; revised manuscript received 11 January 2013; published 13 February 2013)

We report a series of electronic-structure calculations for CrN films within the LDA + U method. In the bulk, it was found previously that with the onset of antiferromagnetic order, a gap opens and an insulating state appears. However, for thin films with increasing thickness (4–10 layers), we find that starting with a critical thickness of 10 (cubic symmetry) or 6 layers (orthorhombic) the gap closes and conducting states appear. The appearance of metallic states is connected with a structural relaxation at the surface, where Cr (N) atoms buckle inside (outside), forming an effective dipole moment. With CrN being a low-gap system, the electric dipoles at the surface caused by the Cr atoms displacing inwards shift the bands around the Fermi level significantly enough to drive those thin films metallic. The potential shift due to these surface dipoles is also visible in Cr and O core-level shifts.

DOI: 10.1103/PhysRevB.87.075114 PACS number(s): 71.20.−b, 73.20.−r, 73.22.−f

I. BACKGROUND

The manipulation of the electronic structure of a material via quantum confinement and dimensionality reduction has attracted much attention recently, becoming one of the most prolific areas in the field of materials science. The properties of such nanomaterials have been shown to be very different from those of their three-dimensional (3D) precursors. In materials with reduced dimensionality, the effects of shapes and boundaries become crucial. For this reason, the observation of surface states in thin-film geometries has drawn much attention. For example, new electronic properties have been observed in oxide heterostructures, unanticipated by those of the bulk constituents[1] with the interface between two nonmagnetic insulating oxides ($LaAlO_3/SrTiO_3$) observed to be conducting,[1] ferromagnetic,[2] and even superconducting.[3] All these properties are believed to occur in a very thin layer around the interface where peculiar two-dimensional (2D) electronic states reside. Surface effects such as those caused by vacancies produced mechanically lead to a 2D electron gas confined to a nanometric surface layer in $SrTiO_3$.[4] In all cases, surface reconstructions lead to new electronic phenomena where all the electronic, spin, and orbital degrees of freedom become active and interact differently than in the case of the bulk.

CrN is a transition-metal nitride (TMN) that has attracted considerable attention due to its interesting physical properties. It shows a magnetostructural phase transition (MPT) as a function of temperature from an orthorhombic antiferromagnetic (AFM) phase to a cubic paramagnetic (PM) one.[5] The AFM configuration is quite unique, showing significant exchange striction induced below the ordering temperature to accommodate the different magnetic bonds in the compound as explained by Filipetti *et al.*[6] using *ab initio* techniques. A recent theoretical work describes the PM phase using *ab initio* molecular dynamics.[7] CrN also exhibits high thermal stability, corrosion resistance, and excellent mechanical properties that have recently been proposed to be susceptible to improvements[8] if somehow one can force the system to remain in the harder AFM configuration. All this combined with the ease of film deposition and promising thermoelectric properties[8–10] make this compound a good source of different physical properties. In spite of its simple structure and the amount of work accumulated over the years, it is still a ground for contention among different pictures, both of its conduction and electronic properties.

The nature of the transition in CrN in terms of the electrical conduction behavior has had a wide range of interpretations in the literature. It has been argued recently[11] that the material as a bulk is always semiconducting, but being very close to a metal-insulator transition, small perturbations such as doping, pressure, or thin-film deposition can drastically change its conduction properties. Claims exist[12] that CrN is a unique case of a 3D-AFM metal, but its conductivity increases with temperature in all stoichiometric bulk samples. We will analyze below the case of thin films in more detail. At the surface of a crystalline solid, the symmetry of the ordered bulk phase is broken. This reduced symmetry allows for new phenomena to be observed, which are not possible in the bulk. As we mentioned above, this has striking consequences even in nonmagnetic wide-gap perovskite oxides. In the case of CrN, the nature of the MPT in thin films is modified with respect to the case of the bulk. Contrary to the case in the bulk, the low-temperature phase is found to be metallic in various works and under different growth conditions. The transition can even be suppressed via N excess[13] and also due to epitaxial constraints,[14–17] suggesting a strong relationship between the transition and the structural properties.

At least three different points of view can be found in literature to describe the nature of the MPT, which we summarize as follows.

Metal to semiconductor. Constantin *et al.*[18] grew CrN(001) thin films on MgO(001) using molecular beam epitaxy. The films show a MPT at 285 K, with activated semiconducting behavior above T_N and a band gap of 0.07 eV. Below the transition temperature, the films are metallic. Nearly stoichiometric polycrystalline films grown by Tsuchiya *et al.* at $P_N = 20\%$ and 30% using reactive sputtering show an AFM first-order phase transition at $T_N \sim 260$ and 230 K, respectively.[13] The reduction of T_N with the N content points out the importance of overstoichiometries in this system. A steep decrease of the

resistivity below T_N is found for the sample grown at 20% (from 260 to 200 K). For the sample prepared at $P_N = 30\%$, the resistivity decreases below 230 K in all the temperature range, showing metallic behavior below T_N. Above T_N, both samples show a small negative temperature coefficient of resistivity, indicative of semiconducting behavior.

Metal to metal. In the study of Inumaru *et al.*,[15] CrN films were epitaxially grown on α-Al_2O_3 (0001) and MgO(001) substrates by pulsed laser deposition. The films grown on α-Al_2O_3(0001) with their (111) planes parallel to the substrate show no structural transition, whereas CrN(001) films grown on MgO(001) show a transition to an AFM state at about 260 K. Both films exhibit metallic T dependence of the resistivity, but a drop in its values below the Néel temperature is observed for the samples showing a MPT. Even bulk samples have been grown showing a structural transition at 240 K with large metallic conductivities, suggesting they are somewhere inside the N-rich heavily doped region.[19] However, a sharp drop in the susceptibility signaling the development of an AFM phase has not been observed in these metallic samples. The reduced bulk modulus observed in those heavily doped CrN samples is consistent with the values reported for metallic TiN rather than CrN, which lies in the more insulating limit.[8] Off stoichiometries are hence a very important factor, difficult to analyze if a proper characterization is not carried out.

Semiconducting behavior. In the above-mentioned work of Tsuchiya *et al.*,[13] overstoichiometric films are always semiconducting and do not show a phase transition. The insulating behavior of those samples grows with the N content. In Ref. 16, single and polycrystalline CrN layers have been grown by reactive sputtering deposition on both MgO and quartz substrates. Epitaxial constraints and the appropriate N content cause single-crystal CrN to remain in the cubic high-temperature phase showing insulating behavior over the whole temperature range.

The importance of the N vacancy concentration as well as the substrate and associated grain boundaries has been recently shown in a experimental work by Duan *et al.*[20] Polycrystalline CrN_x films on Si(100) and glass substrates as well as epitaxial CrN_x films on MgO(100) have been grown by reactive sputtering with different N gas flow rates (f_{N_2}). Both in epitaxial and polycrystalline films there is a transformation of conductance from metallic to semiconducting as f_{N_2} is increased. Only the polycrystalline films prepared at $f_{N_2} = 30$ and 50 sccm show a discontinuity in ρ(T) curves at 260–280 K. While for $f_{N_2} = 30$ sccm the film shows a metal-insulator-like transition, for $f_{N_2} = 50$ sccm the resistivity shows a steep decrease with decreasing temperature in the range 260–280 K and increases with decreasing temperature below 145 K. The transition is absent in all the CrN_x epitaxial films.

In any case, it becomes necessary to elucidate the origin of the experimentally found metallic behavior in the low-temperature phase, whether it can be intrinsic or not, and also what the effects of the material being so close to a metal-insulator transition are when it is nanostructured in the form of thin films. In order to do that, we present here our studies on the electronic and magnetic properties of free-standing CrN thin films by using first-principles electronic-structure methods. Our goal is to analyze the changes in electronic structure with respect to the material as a bulk, determine the relaxed equilibrium structures and the appearance of new electronic states and their origin as a consequence of nanostructuring.

II. COMPUTATIONAL PROCEDURES

Our electronic-structure calculations were performed within density functional theory[21,22] using the all-electron, full potential code WIEN2K (Ref. 23) based on the augmented plane wave plus local orbitals (APW + lo) basis set.[24] For the structural relaxations, we have used the Perdew-Burke-Ernzerhof version of the generalized gradient approximation(GGA).[25]

To deal with strong correlation effects, we apply the LDA + U scheme[26] that incorporates an onsite Coulomb repulsion U and Hund's rule coupling strength J_H for the Cr 3d states. The LDA + U scheme improves over GGA or LDA in the study of systems containing correlated electrons by introducing the onsite Coulomb repulsion U applied to localized electrons. We have performed calculations on CrN within the LDA + U method (using the so-called fully localized version for the double-counting correction), taking a $U = 4$ eV value for CrN. Such a value has been shown to be reliable for CrN bulk[11,27] based on the agreement with photoemission experiments and transport properties, the comparison between band-structure parameters and optical data, and a comparison with parameter-free functionals. The onsite Hund's exchange parameter J_H was set to zero. In Ref. 28 it is claimed that bulk CrN is better described within LDA+U with a slightly smaller U value of 3 eV by comparing the calculated structural parameters with the experimental values and the density of states with the available photoemission spectra. However, the calculated cubic lattice parameter obtained within GGA agrees nicely with the common value found experimentally in Refs. 8 and 29. Since U could in principle vary significantly on a surface, we have chosen a truly *ab initio* GGA scheme for the structural relaxations.

All calculations were fully converged with respect to all the parameters used. In particular, we used $R_{\rm mt}K_{\rm max} = 7.0$, and muffin-tin radii of 1.95 a.u. for Cr, and 1.73 a.u. for N.

III. RESULTS

Unit-cell details. We investigate the changes in the electronic structure that occur when nanostructuring CrN in the form of free-standing thin films. We have modeled 4-, 6-, 8-, and 10-layer thick films grown along the (001) direction starting from both the experimentally observed low-temperature orthorhombic and the high-temperature cubic (rocksalt) bulk unit cells. For all the cases, we have performed calculations keeping the bulk positions fixed (nonrelaxed cases) or with fully relaxed atomic positions (relaxed cases). Cubic lattice parameters would be the situation of a film on top of a cubic substrate whereas the orthorhombic lattice parameters would allow the relief of exchange-related stress. For the orthorhombic unit cell, the optimized bulk cell parameters used as a starting point to create the supercells were $a = 5.774$ Å, $b = 2.973$ Å, $c = 4.146$ Å. For the cubic films, we have used as a starting point the experimental cell parameter obtained by Corliss *et al.*[5]: $a = 4.134$ Å. A vacuum of 15 Å was used for all the calculations, after checking that it is enough to guarantee the lack of interaction between CrN blocks [see

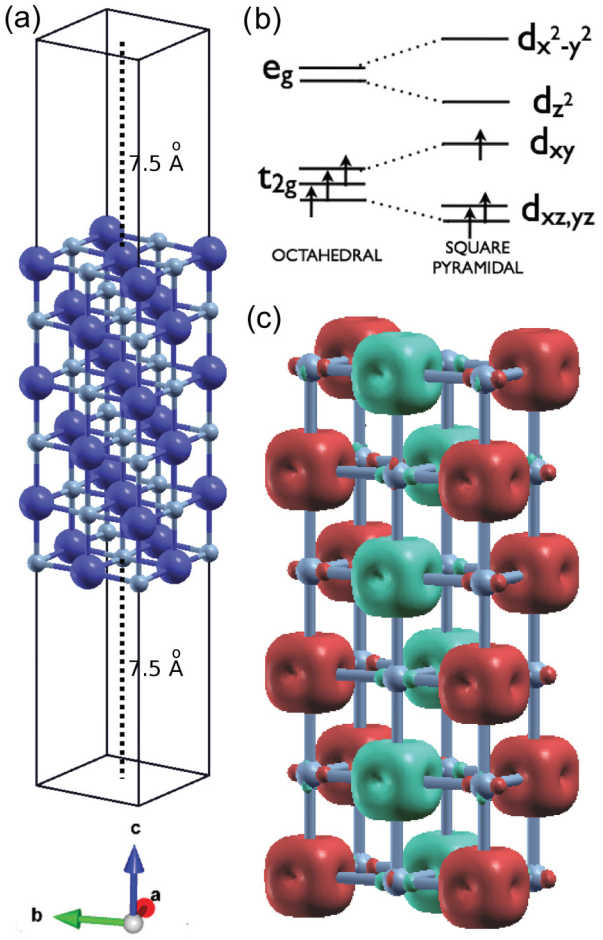

FIG. 1. (Color online) (a) Unit cell of the orthorhombic six-layer CrN film with the N atoms (smaller) in gray and the Cr atoms (larger) in blue. (b) Level schemes representing the electronic structure of a Cr^{3+} cation in an octahedral environment (left) and in a square pyramidal one (right). The splitting of both e_g and t_{2g} levels in a square pyramidal environment can be observed. (c) Three-dimensional plot showing the difference between the spin-up and spin-down (different color/grayscale) electron densities. The in-plane AFM order chosen for the calculations can be seen. The typical $d^3(t_{2g}$-like) electronic configuration of each Cr^{3+} cation and the small magnetic polarization of the neighboring ligands can be observed.

Fig. 1(a)]. In-plane AFM order was imposed and in order to allow for this type of ordering within one plane, an in-plane $\sqrt{2} \times \sqrt{2}$ supercell was constructed. Note that this imposed in-plane checkerboard AFM ordering is not the bulk CrN (AFM2) structure since this would require larger supercells. However, we have checked other magnetic structures (such as G type) and the effects of a particular magnetic order on our conclusions in this paper are minor.

Ionic model. Since the compound is a moderately correlated TMN, a crude estimate of the possible electronic configuration of the material can be obtained from an ionic model. Two different types of Cr environments should be distinguished: octahedral for the inner Cr atoms and square pyramidal for the surface Cr atoms. In a square pyramidal environment caused at the surface by the absence of one apical nitrogen (surface termination is depicted in Fig. 1), the degeneracy of the octahedral t_{2g} levels is lifted with the $d_{xz,yz}$ orbitals lying lower in energy. The degeneracy of the e_g levels is also lifted, lowering in energy the d_{z^2} orbital [see Fig. 1(b)]. Taking the usual valence for N, the average valence for the Cr cations is $+3$. The electronic configuration as well as the chosen in-plane AFM order can be observed in Fig. 1(c). Significant contribution of the N p bands below the Fermi level is expected due to hybridization of these states with the Cr d bands. For both the octahedral and square pyramidal Cr atoms in a high-spin state ($S = \frac{3}{2}$, magnetic moment of 3 μ_B), the orbitals $d^{\uparrow}_{xz,yz,xy}$ are completely filled, while the minority $d^{\downarrow}_{xz,yz,xy}$ remain empty, with the $d_{x^2-y^2,z^2}$ states for both spin channels also completely empty above the Fermi level. The competition between crystal-field splitting and Hund's rule coupling strength will dictate what the first unoccupied states are (whether $t^{\downarrow}_{2g}$ or $e^{\uparrow}_{g}$). Moreover, at the surface, it is important to understand the relative value of the splittings within the t_{2g} and e_g multiplets due to the reduced symmetry, with respect to the Hund's rule coupling strength and the octahedral t_{2g}-e_g crystal-field splitting. These values could be such that there exist band crossings and metallic states arising due to the surface coordination of the Cr atoms. Just focusing on the majority spin channel, if the t_{2g}-e_g crystal-field splitting is on the order of the splittings inside the t_{2g} and e_g manifolds caused by the surface dangling bonds, bands coming from the surface Cr atom could cross at the Fermi level, leading to a conducting state with strong surface Cr d character. This would be an interesting conducting state confined to the surface. However, we will see below that crystal-field splittings at the surface are not the only effect that displaces the bands with respect to the bulk case; the effects of surface atomic relaxations play a role as well in very thin films.

Evolution with thickness. CrN with an in-plane AFM ordering is a low band-gap material. Eventually, nanostructuring in thin films will reorganize the bands around the Fermi level, with the possible appearance of surface states, as we described above. It is interesting to analyze the evolution of the band gap and the band structure in general in the different structures we have calculated. Looking at Table I, one can see that the tendency of the films towards metallicity is increased by the

TABLE I. Band-gap values (in meV) for CrN bulk and thin films of different thicknesses obtained within the LDA + U method (U = 4 eV) using an in-plane AFM order (both for the nonrelaxed and the relaxed positions) using the cubic and orthorhombic bulk unit cells. In the insulating cases, the band gap is obtained as the difference between the eigenvalues at Γ (bottom of the conduction band) and M (top of the valence band). In the metallic cases, the degree of metallicity is measured as the same difference (in that case with negative value).

	Number of layers				
	Bulk	4	6	8	10
Cubic					
Nonrelaxed	200	119	128	122	113
Relaxed		206	195	19	−100
Orthorhombic					
Nonrelaxed	170	4	18	16	10
Relaxed		34	−14	−170	−225

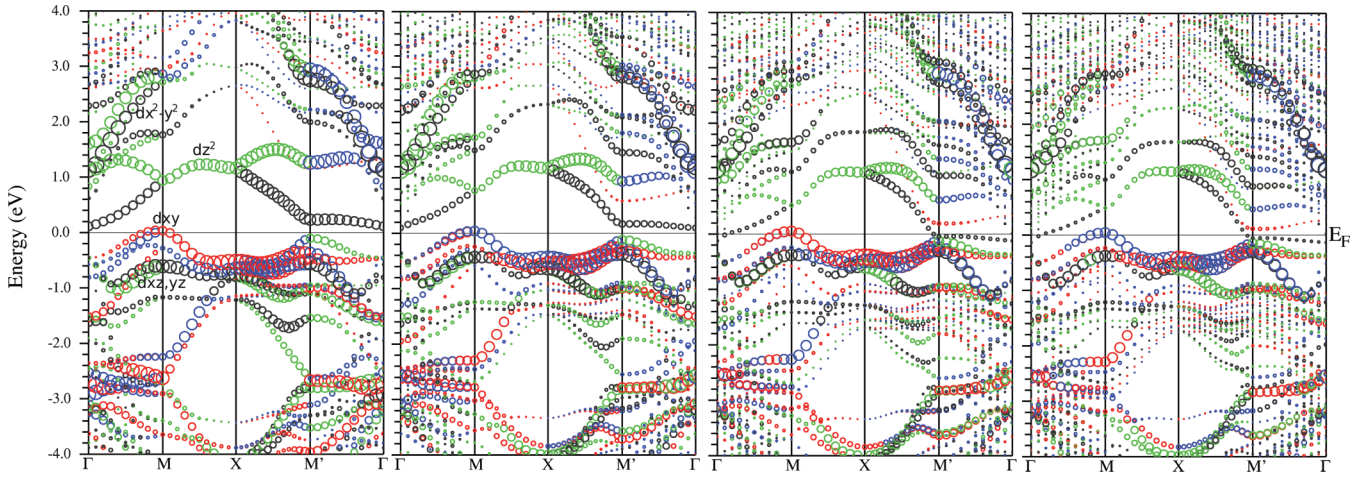

FIG. 2. (Color online) Band structures with band character plot (surface Cr atom highlighted) for orthorhombic CrN films of 4, 6, 8, and 10 layers (from left to right) and relaxed positions. The size of the circles is proportional to the surface Cr character of the corresponding eigenstate. The colors indicate the irreducible representation of the eigenvalues. Whenever two bands cross, the connectivity of the band crossing can be seen just following the color of the band.

orthorhombic distortion. In the insulating cases, the band gap can be obtained as the difference between the eigenvalues at Γ (bottom of the conduction band) and M (top of the valence band). If we keep this picture in mind, the evolution of the band gap can be extended to the metallic phase as the same difference between eigenvalues, but in that case with negative values. Hence, it can be seen how, for the cubic case, the relaxed 10-layer film is metallic and for the orthorhombic ones, already the 6-layer film is metallic with the tendency towards metallicity increasing as the number of layers does (with a band gap of -14 meV for the 6-layer case and -225 for the 10-layer one). The values of the band gap are always one order of magnitude higher for the cubic structures with respect to the orthorhombic ones. The nonrelaxed structures remain insulating for both the cubic and orthorhombic films, although the last ones are closer to metallicity with very small values of the band gap (from 4 to 18 meV). The structural relaxation increases the band gap for the thinner films (for the four-layer cubic case, from 119 to 206 meV and for the orthorhombic, from 4 to 34 meV) and drastically decreases it for the thicker films. It is interesting to note that, contrary to most other correlated insulators, a structural relaxation does not favor the opening of a gap in the case of CrN thin films. This is quite peculiar and suggests that the formation of conducting states in a thin-film geometry is particularly favored energetically and will be directly connected to surface reconstructions. We will see in the following that the four-layer system is different because being so thin, the structural relaxations do not allow for an accommodation of the surface Cr in its five-neighbor environment as it does for the thicker films.

The evolution of the band structure within the LDA + U method ($U = 4$ eV) with film thickness using the fully relaxed positions for the orthorhombic (distorted) structure is presented in Fig. 2. We have chosen an in-plane k path $\Gamma(0,0,0)$-$M(\pi/a,0,0)$-$X(\pi/a,\pi/b,0)$-$M'(0,\pi/b,0)$-Γ. The band-gap evolution with thickness we have analyzed in Table I can be seen, closing as the number of unit cells increases. The most noticeable features arising in these band-structure plots are the surface states appearing below the Fermi level. The surface Cr d character of the bands is marked in Fig. 2. Due to the dangling bonds (lack of apical nitrogens) around the Cr atoms at the surface, the Cr d levels split as sketched in Fig. 1(b): the t_{2g} triplet with the $d_{xz,yz}$ doublet lying lower in energy completely occupied below the Fermi level, the d_{xy} singlet also occupied but split with respect to the $d_{xz,yz}$; the e_g bands present the d_{z^2} also split with respect to the $d_{x^2-y^2}$, with the latter lying higher in energy. Another feature is that the surface Cr energy bands lie higher in energy than those of the inner ones, well separated due to a surface effect (we will analyze this below in detail). Let us focus on the M point and its evolution as the thickness is increased to the right of Fig. 2. The highest occupied valence band has always surface Cr d character, but not so the lowest-lying unoccupied conduction band. In addition, there is a flattening of the dispersion of this conduction band from Γ to M and more so from M' to Γ (even crossing the Fermi level in the 10-layer case at the same time that it loses most of its surface Cr character). For the X point, however, a large surface Cr d character is always retained. As the thickness increases, the difference in bandwidth between more inner layers and the surface one (smaller coordination) becomes more noticeable, eventually producing the band crossings at the Fermi level that we observe for the 8- and 10-layer cases. Although the shape of the bands right below the Fermi level is almost the same for all the thicknesses calculated, in the Γ-M direction a different feature can be observed in the four-layer (the thinner) case: the first two bands right below the Fermi level (of d_{xy} character and corresponding to the two surfaces) are split. The reason is that the distance between the two surfaces is not big enough and they actually interact through the CrN bulk (two-layer thick only) barrier leading to a bonding-antibonding splitting. Even for the six-layer case, a very small splitting along the same direction can be seen (particularly near the M point), but no splitting can be observed either in the 8-layer or in the 10-layer case, indicating the thickness of the film in these cases

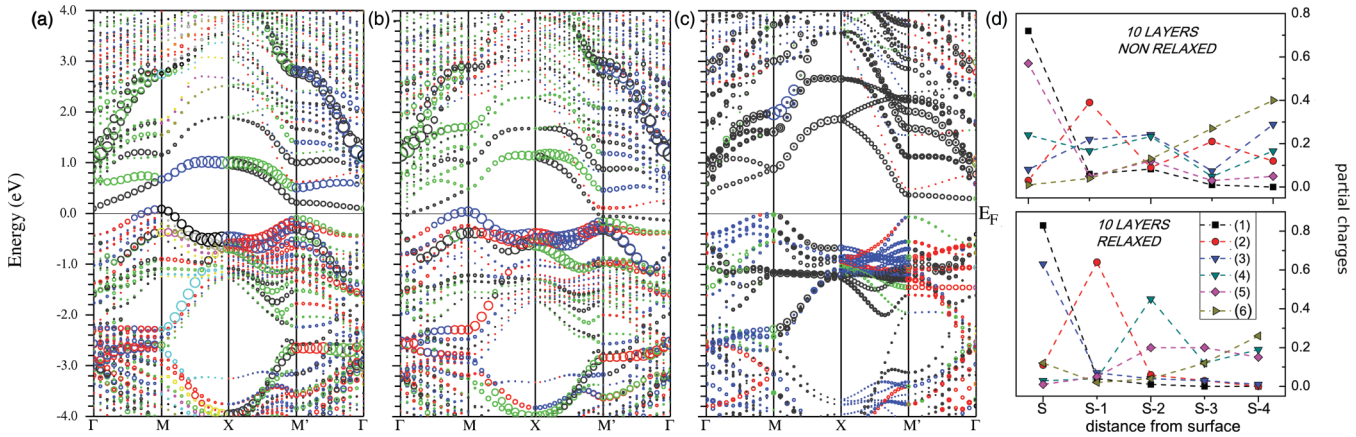

FIG. 3. (Color online) Band structures with band character plot for the surface Cr atom in 10-layer thick CrN films within the orthorhombic structure (a) keeping the bulk positions fixed, (b) relaxing the atomic positions, and (c) without vacuum [in the (c) panel, the character of the same atoms as in (a) and (b) is highlighted but of course there is no surface anymore since there is no vacuum]. The (d) panel shows the sum of the partial charges of the atoms in each layer [from surface (S) to inner (S-n)] for the first six eigenvalues at M right below the Fermi level [(1) being the highest one] for both relaxed and nonrelaxed structures.

is enough to guarantee the lack of interaction between the two surfaces across the CrN inner layers.

10-layer case in detail. We will now focus on the 10-layer case to see the changes that happen when the atomic positions within the film are fixed at the bulk positions and also when relaxed. We have already mentioned that lattice relaxations lead to conducting states in these thin films. In order to check if these states right below the Fermi level with high-surface Cr character are actually surface states, we have removed the vacuum (recovering the bulk solution but keeping the symmetries present in the films) and performed calculations in the same conditions (LDA + U, $U = 4$ eV). The three band-structure plots (nonrelaxed and relaxed positions and vacuum suppressed) are shown in Fig. 3 with the surface Cr bands highlighted. For the nonrelaxed case, the surface bands right below the Fermi level can be seen. These bands remain almost the same in the relaxed case (although with higher contribution from the surface Cr in the M'-Γ direction). In both cases, a very flat band appears in the M-X-M' direction at about -3.5 eV. The main contribution to this band comes from the surface N atom as a consequence of the hybridization of the N-p states with the Cr-e_g-like ones. In both cases, there is a considerable contribution of the surface N atom to the surface bands, particularly in the Γ-M direction.

Let us see the main difference between the relaxed and the nonrelaxed cases focusing on the bands around the Fermi level. In the nonrelaxed case, the character of the band gap is clearly surfacelike (d_{xy}-d_{z^2}) since most of the contribution to both the bands right above and below the Fermi level comes from the surface Cr atom. However, when the atomic positions are relaxed, the solution is metallic, and the character of the first band right above the Fermi level at M changes to the more inner Cr atoms. The first band right below the Fermi level at M being of surface Cr d_{xy} character and the first right above of innermost Cr d_{z^2} character. Comparing with the case without vacuum, the curvature of the bands right below the Fermi level is different from the case with vacuum, indicating that the bands are different. As expected, the surface states shown in Figs. 3(a) and 3(b) no longer appear since there is no surface. In addition, the bands right below the Fermi level for the case without vacuum are not occupied by the interfacial Cr atom, but by more inner ones.

The right panel in Fig. 3 shows the sum of the partial charges of the atoms (Cr + N) in each layer [from surface (S) to inner (S-n) layers] for the first six (numbered 1 to 6, 1 being the highest one in energy) eigenvalues at M right below the Fermi level for the cases with a vacuum. This plot gives further confirmation of the surface character of the bands right below the Fermi level [shown in Figs. 3(a) and 3(b)]. There are two eigenvalues whose highest partial charge comes from the surface. For those states, the value of the partial charges as a function of the layer decays rapidly as one moves away from the surface. Eigenvalue (2) is fairly delocalized in the nonrelaxed case, but gets more localized in the S-1 layer (and a bit in S) after the relaxation. However, for the other eigenvalues, the character of the partial charge is much more oscillating in the different layers, suggesting that those states are more bulklike states. Again, we see how the surface states are more localized than those in the more inner layers away from the surface.

Concerning the magnetic moments of Cr ions, the values are in-between those reported experimentally (2.36 and 3.17 μ_B).[5,30] Values of the magnetic moment inside the Cr muffin-tin spheres chosen change from 2.63 μ_B for the surface Cr to 2.57 μ_B for the inner ones in the case of the nonrelaxed structures. For the relaxed structures, the magnetic moment of the surface Cr is around 2.53 μ_B and 2.50 μ_B for the other Cr atoms. Relaxations distribute moments more evenly, but still surface Cr atoms always have larger moments.

Influence of lattice relaxations: Surface dipole formation. The lattice relaxations were obtained within GGA allowing a displacement of the atoms along the z direction. Looking at the average distances between planes shown in the inset of Fig. 4 at first we notice a Friedel-type surface relaxation where the surface atoms relax inwards (average distance to the S-1 plane only 2.03 Å), but the distance between the S-1 and S-2 layers

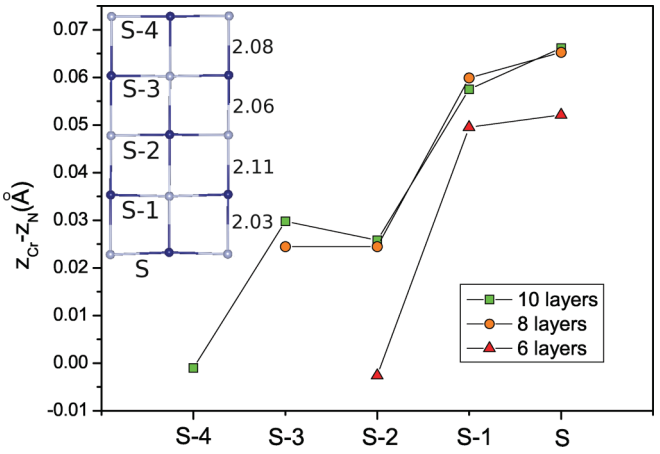

FIG. 4. (Color online) Vertical displacements of N anions with respect to Cr cations ($\Delta z = z_{Cr} - z_N$) in CrN films 6-,8-, and 10-layer thick obtained within GGA. The abscissa axis shows the distance from the surface in terms of number of layers (S-n). The inset shows half a unit cell of the relaxed 10-layer structure with the Cr atoms in blue (darker) and the N atoms in gray (lighter). The buckling of the octahedra/pyramids (particularly at the surface) can be observed. The average distances between layers along the z axis (in Å) are also shown.

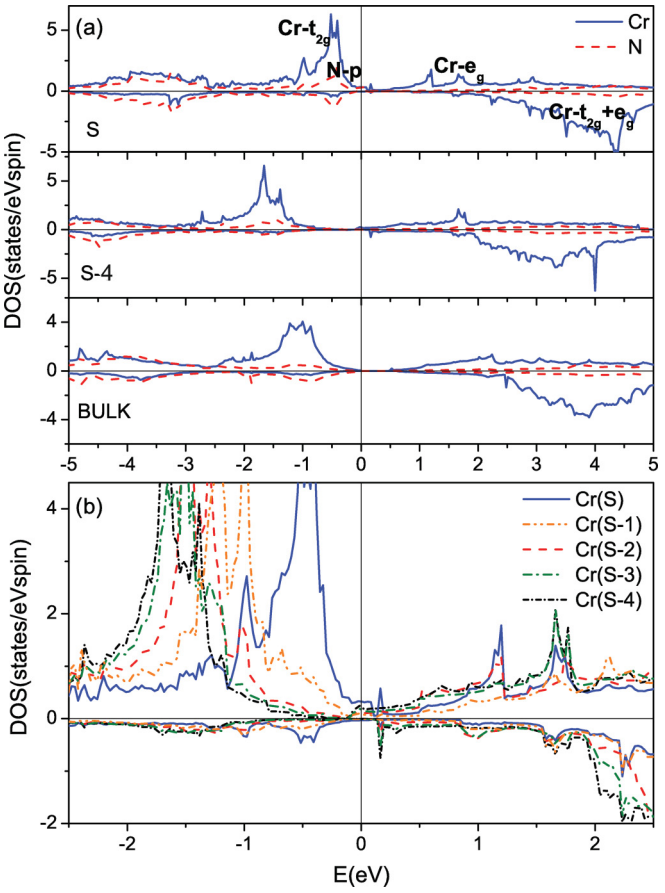

FIG. 5. (Color online) Density of states in the orthorhombic 10-layer CrN film with relaxed atomic positions of (a) the Cr and N atoms for the surface (S) and central (S-4) layers and, (b) the Cr atoms in each layer [from surface (S) to center (S-n)]. The Fermi energy is set at zero. The positive and negative values are for spin up and spin down, respectively. The density of states of Cr and N atoms in bulk CrN is also shown in the (a) panel.

increases to 2.11 Å and the bulk distance (2.08 Å) is reached in an oscillatory way. Atomic displacements from the ideal rocksalt structure that affect Cr cations and N anions in the same way will give no net lattice polarization. However, if the displacements are different for cations and anions, they have a polar character and will result in the appearance of a local electric field that should displace the bands to higher energies where the field is bigger. The difference in displacements experienced by Cr/N atoms for each layer is shown in Fig. 4. The largest displacements are always observed at the surface, where the differences in the electronic distribution are also larger due to the dangling bonds. The absence of an apical N forces the Cr atoms at the surface to relax inside the N pyramid formed by its five anion neighbors. Thus, the surface CrN plane has higher N character, being the Cr atoms slightly lower in height, away from the surface. This type of surface relaxation pattern has been obtained in the past for the (001) surface of other TMN (VN and TiN).[31] This will lead to a net polarization near the surface and to some degree could lead to the appearance of a negatively charged plane caused by the higher density of N^{3-} anions at the surface. In any case, it can be seen that the difference in displacement of Cr and N atoms is reduced away from the surface towards the inner layers. For 10 and 6 layers, Fig. 4 shows that the differences in the positions of Cr and N atoms for the central layers are almost negligible. The displacements are a clear indication of the potential being different for the surface atoms due to the dangling bonds.

Those ionic displacements and the redistribution of electrostatic potential near the surface will have consequences in the band structure. In order to analyze the distribution of electronic states around the Fermi level and their shift in energy with respect to the more inner layers, we have plotted in Fig. 5 the density of states (DOS) of Cr and N atoms in the 10-layer relaxed film. In Fig. 5(a), it can be seen that the t_{2g}-like, $d^{\uparrow}_{xz,yz,xy}$ orbitals [degenerate for the inner (S-4) Cr atom and with this degeneracy lifted at the surface (S)] are filled (in the range between -2 and 0 eV below the Fermi energy). A small amount of (bonding) e_g levels (in the range between -6 and -3 eV) are occupied for every Cr atom. Comparing the surface (S) and central (S-4) DOS of Cr atoms, an upward shift of the Cr-t_{2g}-like bands of about 1 eV towards the Fermi level is observed (similar for the e_g's but more difficult to observe due to their larger bandwidth). In Fig. 5(b), the features around the Fermi level can be distinguished: the metallic character (nonzero DOS at the Fermi level) and the larger contribution of the surface (S) Cr at E_F. It can also be seen that the upward shift is nearly rigid from layer to layer as the surface is approached: the inner the Cr atom is, the lower in energy the occupied $t^{\uparrow}_{2g}$-like and the unoccupied e_g manifolds are. This is consistent with the shift in potential as the surface is approached caused by the change in environment and the appearance of a surface dipole moment. We should clarify here that this situation is different to a potential buildup in polar interfaces, it is just a surface effect caused by dangling bonds at the surface. It will not be a cumulative effect as more layers are added up. In fact, the opposite is true: it should be more

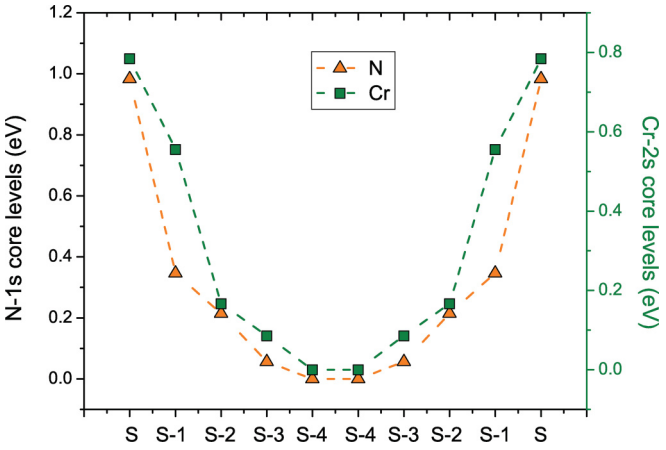

FIG. 6. (Color online) Energy difference of the N 1*s* and Cr 2*s* core level in the 10-layer case CrN film compared with the value of the central layer.

important for thinner layers, where the surface-to-volume ratio is higher and the surface states have a higher relative weight.[32] Also, it becomes important in low-gap semiconductors such as CrN, but (although still present) should be much less so for higher-gap ionic semiconductors such as $SrTiO_3$, TiO_2, etc.

This can be analyzed more quantitatively using the shift in core-level energies (Cr 2*s* and N 1*s*) shown in Fig. 6. A shift of about 1 eV upwards as the surface is approached is observed here in Fig. 6 (core-level energies) as it was also in Fig. 5 (DOS). The electrons at the surface are less bound due to the absence of some ligands, which leads to a higher localization of their bands (smaller bandwidths), and also higher core-level energies caused by the local electric field produced by the atomic displacements we described above. Also, the broken symmetry reduces the crystal-field splittings and leads to a small increase in magnetic moment (that we quoted above). In metallic solutions, if an ionic picture is still possible, one can argue that the lack of N^{3-} apical neighbors reduces the valence of the surface Cr atoms, leading to a larger magnetic moment. Being the system almost in the localized limit, with very small charge redistribution among bands, the effect is small but still noticeable in the calculations.

IV. SUMMARY

We have studied the appearance of surface states in thin CrN films due to the dangling bonds caused by the lack of apical N atoms at the surface. These states become further stabilized by structural relaxations, which tend to favor a gap closure and hence a metallic solution for the system. Metallicity is not confined to the surface, hence, this effect could contribute to the metallicity observed experimentally, at least in the case of very thin films and below the MPT. The band-gap closure comes about due to the displacements of the ions at the surface, where an electric field is formed, with the corresponding band shifts, as high as 1 eV. The nonrelaxed cases remain insulating because the atomic relaxations that lead to such a local electric polarization are suppressed. This suggests that local strains and other defects can drastically modify the conduction properties of CrN as it is observed experimentally.

ACKNOWLEDGMENTS

The authors thank the Ministerio de Educación y Ciencia (MEC) for the financial support through the Project No. MAT2009-08165. A. S. Botana and V. Pardo thank the Spanish Government for financial support through the FPU and Ramón y Cajal Program, respectively. P. Blaha thanks the Austrian Science Fund for financial support (Project No. SFB-F41, ViCoM).

*Corresponding author: antia.sanchez@usc.es

[1] A. Ohtomo and H. Hwang, Nature (London) **427**, 423 (2004).
[2] A. Brinkman, M. Huijben, M. van Zalk, J. Huijben, U. Zeitler, J. C. Maan, W. G. van der Wiel, G. Rijnders, D. H. A. Blank, and H. Hilgenkamp, Nat. Mater. **6**, 493 (2007).
[3] N. Reyren, S. Thiel, A. D. Caviglia, L. F. Kourkoutis, G. Hammerl, C. Richter, C. W. Schneider, T. Kopp, A.-S. Retschi, D. Jaccard *et al.*, Science **317**, 1196 (2007).
[4] A. F. Santander-Syro, O. Copie, T. Kondo, F. Fortuna, S. Pailhes, R. Weht, X. G. Qiu, F. Bertran, A. Nicolaou, A. Taleb-Ibrahimi *et al.*, Nature (London) **469**, 189 (2011).
[5] L. M. Corliss, N. Elliott, and J. M. Hastings, Phys. Rev. **117**, 929 (1960).
[6] A. Filippetti and N. A. Hill, Phys. Rev. Lett. **85**, 5166 (2000).
[7] P. Steneteg, B. Alling, and I. A. Abrikosov, Phys. Rev. B **85**, 144404 (2012).
[8] F. Rivadulla, M. Bañobre-López, C. X. Quintela, A. Piñeiro, V. Pardo, D. Baldomir, M. A. López-Quintela, J. Rivas, C. A. Ramos, H. Salva *et al.*, Nat. Mater. **8**, 947 (2009).
[9] C. X. Quintela, F. Rivadulla, and J. Rivas, Appl. Phys. Lett. **94**, 152103 (2009).
[10] C. X. Quintela, F. Rivadulla, and J. Rivas, Phys. Rev. B **82**, 245201 (2010).
[11] A. S. Botana, F. Tran, V. Pardo, D. Baldomir, and P. Blaha, Phys. Rev. B **85**, 235118 (2012).
[12] P. A. Bhobe, A. Chainani, M. Taguchi, T. Takeuchi, R. Eguchi, M. Matsunami, K. Ishizaka, Y. Takata, M. Oura, Y. Senba *et al.*, Phys. Rev. Lett. **104**, 236404 (2010).
[13] Y. Tsuchiya, K. Kosuge, Y. Ikeda, T. Shigematsu, S. Yamaguchi, and N. Nakayama, Mater. Trans., JIM **37**, 121 (1996).
[14] D. Gall, C.-S. Shin, R. T. Haasch, I. Petrov, and J. E. Greene, J. Appl. Phys. **91**, 5882 (2002).
[15] K. Inumaru, K. Koyama, N. Imo-oka, and S. Yamanaka, Phys. Rev. B **75**, 054416 (2007).
[16] X. Y. Zhang, J. S. Chawla, R. P. Deng, and D. Gall, Phys. Rev. B **84**, 073101 (2011).
[17] X. Y. Zhang, J. S. Chawla, B. M. Howe, and D. Gall, Phys. Rev. B **83**, 165205 (2011).

[18]C. Constantin, M. B. Haider, D. Ingram, and A. R. Smith, Appl. Phys. Lett. **85**, 6371 (2004).
[19]S. Wang, X. Yu, J. Zhang, M. Chen, J. Zhu, L. Wang, D. He, Z. Lin, R. Zhang, K. Leinenweber *et al.*, Phys. Rev. B **86**, 064111 (2012).
[20]X. F. Duan, W. B. Mi, Z. B. Guo, and H. L. Bai, J. Appl. Phys. **113**, 023701 (2013).
[21]P. Hohenberg and W. Kohn, Phys. Rev. **136**, B864 (1964).
[22]R. O. Jones and O. Gunnarsson, Rev. Mod. Phys. **61**, 689 (1989).
[23]K. Schwarz and P. Blaha, Comput. Mater. Sci. **28**, 259 (2003).
[24]E. Sjöstedt, L. Nordström, and D. J. Singh, Solid State Commun. **114**, 15 (2000).
[25]J. P. Perdew, K. Burke, and M. Ernzerhof, Phys. Rev. Lett. **77**, 3865 (1996); **78**, 1396(E) (1997).
[26]A. I. Liechtenstein, V. I. Anisimov, and J. Zaanen, Phys. Rev. B **52**, R5467 (1995).
[27]A. Herwadkar and W. R. L. Lambrecht, Phys. Rev. B **79**, 035125 (2009).
[28]B. Alling, T. Marten, and I. A. Abrikosov, Phys. Rev. B **82**, 184430 (2010).
[29]P. S. Herle, M. S. Hedge, N. Y. Vasathacharya, S. Philip, M. V. R. Rao, and T. Sripathi, J. Solid State Chem. **134**, 120 (1997).
[30]R. M. Ibberson and R. Cywinski, Physica B (Amsterdam) **180-181**, 329 (1992).
[31]D. Gall, S. Kodambaka, M. A. Wall, I. Petrov, and J. E. Greene, J. Appl. Phys. **93**, 9086 (2003).
[32]S. Xiao, D. Wei, and X. Jin, Phys. Rev. Lett. **109**, 166805 (2012).